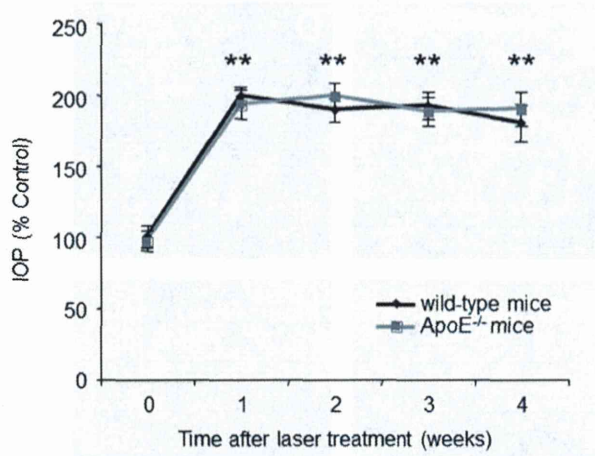

Fig. 2 – Time course of IOP change after laser-induced ocular hypertension ($n=8$) both in wild-type and ApoE$^{-/-}$ mice. IOP was measured at the indicated time points using an applanation tonometer. Data express % vs. control. There were no differences between the wild-type and ApoE$^{-/-}$ mice. **$P<0.01$ compared to control.

significantly lower in the WT mice than in the ApoE$^{-/-}$ mice (1728.4±170.6 cells/mm^2 and 2562.7±141.0 cells/mm^2, respectively, p=0.034, Fig. 5). This neuroprotective effect of ApoE deficiency was still active 14 days after NC, with the WT mice still having a significantly lower density of surviving RGCs than the ApoE$^{-/-}$ mice (528.9±125.4 cells/mm^2 and 1905.9±238.5 cells/mm^2, respectively, $p=0.004$, Fig. 5).

2.4. *NC-induced RGC death through the kainite pathway in WT mice*

In rats, glutamate receptor signaling has been implicated in the NC-induced RGC death (Schmitt and Sabel, 1996; Schuettauf et al., 2000). To further investigate the mechanism of ApoE deficiency's neuroprotective effect in the RGCs, we performed NC in WT mice and simultaneously administered one of two glutamate receptor inhibitors, CNQX and MK801, or PBS. Seven days later, we found that CNQX, an inhibitor of KA receptors, had a significant neuroprotective effect against NC-induced RGC death (PBS: 1728.4±170.6 cells/mm^2, CNQX: 3031.6±246.9 cells/mm^2, $p=0.020$, Fig. 6), but MK801, an inhibitor of NMDA receptors, did not (1769.6±211.9 cells/mm^2, $p=0.663$).

2.5. *Reduced susceptibility to KA toxicity in ApoE$^{-/-}$ mice*

To investigate the susceptibility of ApoE$^{-/-}$ mice to KA toxicity, we injected graded concentrations of KA (0.1, 1, and 10 nmol/eye) or a control (PBS) intravitreally and counted the density of FG-labeled RGCs in both WT and ApoE$^{-/-}$ mice after 7 days. There was no difference in the density of FG-labeled RGCs in the WT mice injected with PBS or 0.1 nmol/eye of KA. However, there was a significantly higher number of surviving RGCs in the ApoE$^{-/-}$ mice than the WT mice after we administered 1 nmol/eye of KA (WT mice: 2719.8±204.9 cells/mm^2, ApoE$^{-/-}$ mice: 4279.2±471.4 cells/mm^2, $p=0.004$) or 10 nmol/eye of KA (WT mice: 797.6±109.1 cells/mm^2, ApoE$^{-/-}$ mice: 1363.3±222.8 cells/mm^2, $p=0.021$; Fig. 7).

3. Discussion

Although ApoE is believed to contribute to the pathophysiology of glaucoma (Lam et al., 2006; Mabuchi et al., 2005; Ressiniotis et al., 2004; Zetterberg et al., 2007), its exact role remains unclear. In this study, we examined the distribution of ApoE and found that it was located in the astrocytes and Müller cells of the retina and in the astrocytes of the optic nerve (Fig. 1). We also found evidence that the RGCs in the ApoE-deficient mice were resistant to death induced by elevated IOP both in the retina (Fig. 2) and in the optic nerve (Fig. 3). To further investigate the mechanism of neuroprotection due to ApoE deficiency, we performed a NC procedure in ApoE-deficient and WT mice to direct our focus on the axonal injury that is believed to contribute to the RGC death in OH (Nakazawa et al., 2006). We found that the ApoE-deficient mice also had a significant resistance to NC-induced RGC death. In WT mice, RGC death following NC was mediated in part by the KA receptor signaling. Since the ApoE-deficient mice were also resistant to KA-induced excitotoxicity, it is probable that the lack of ApoE inhibited the KA receptor signaling. Thus, this is the first report to demonstrate the critical role of ApoE in axonal damage-induced RGC death in mice, and to show that the mechanism of this role probably involved the inhibition of the cytotoxic KA pathway.

In this study, we used laser-induced OH in mice as a model of glaucoma. Previously, the DBA/2J mouse line was established to have a spontaneous mutation that leads to glaucoma, and the use of these mice has contributed greatly to research in this field (Libby et al., 2005a). However, there are limitations to this model, including delayed RGC loss and a considerable inter-individual variability. Moreover, use of this mouse line precludes the use of genetically altered mice. On the other hand, a laser-induced OH model of glaucoma allows high IOP to be rapidly and reliably induced in genetically altered mice, key advantages for investigating the role of target genes (Nakazawa et al., 2006). Here, we found that both OH-induced axonal degeneration and cell body loss were mitigated in ApoE-deficient mice. Furthermore, previous research has shown that the loss of the RGC soma and the loss of the RGC axons have different mechanisms, and that Bax deficiency prevents the former but not the latter (Libby et al., 2005b). This implies that the neuroprotective effect of ApoE deficiency is related to both OH-induced axonal degeneration and RGC loss.

As glaucoma has heterogeneous risk factors, we have previously used several different methods to mimic the human pathogenesis of glaucoma in mice and investigate the mechanism of RGC death: induced OH (Nakazawa et al., 2006), NC (Himori et al., 2013), vinblastine-induced blockage of axoplasmic flow (Ryu et al., 2012), excitotoxicity (Nakazawa et al., 2007b), and hyperglycemia (Shanab et al., 2012). We reported that OH-induced axonal degeneration occurred in part through the up-regulation of TNFα and subsequent microglial activation (Nakazawa et al., 2006), and that axonal damage-induced RGC death was related to oxidative stress

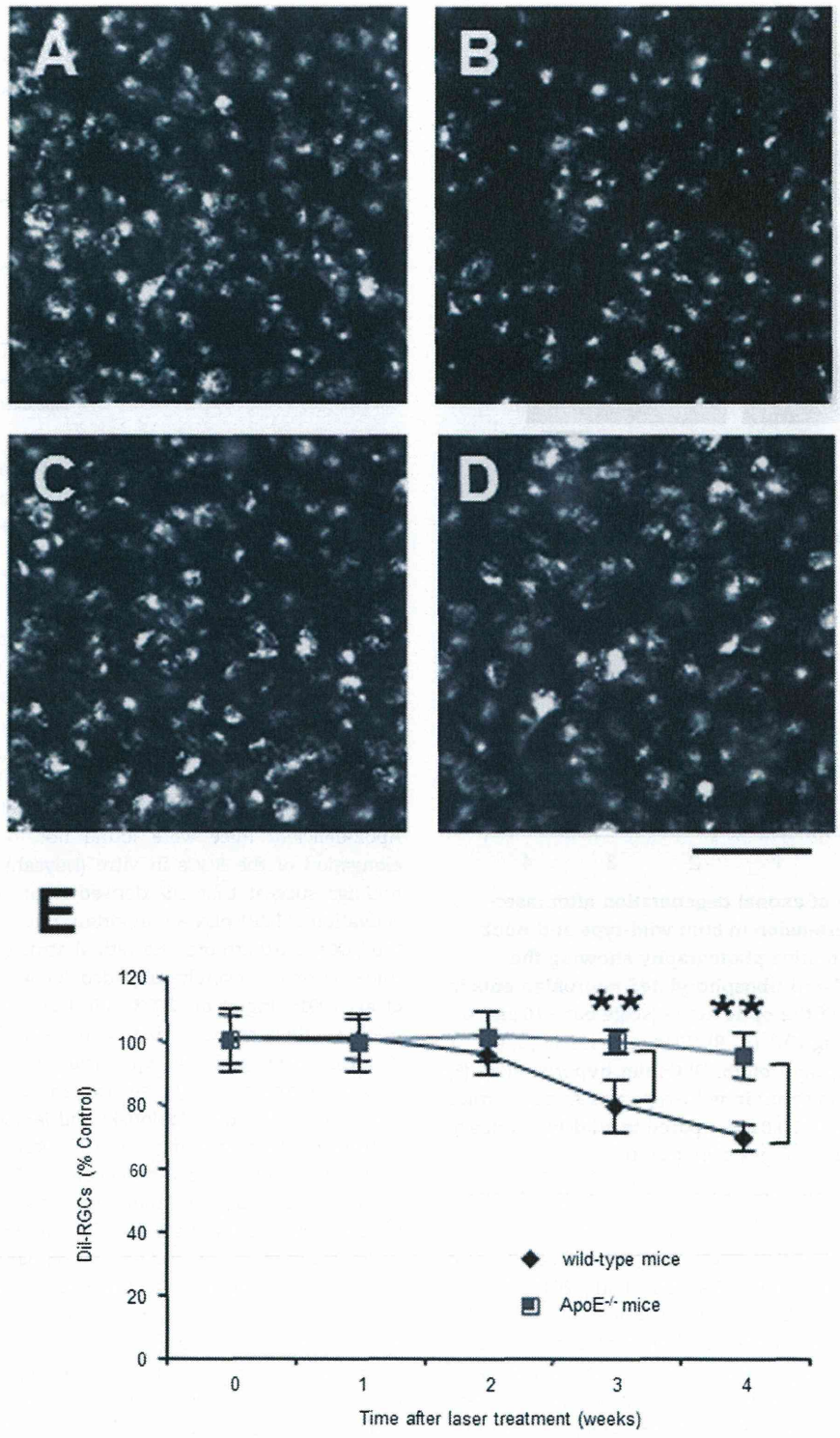

Fig. 3 – Time course of change in Di-I-labeled RGCs after laser-induced ocular hypertension in both wild-type and ApoE$^{-/-}$ mice (A-D) Representative photographs of Di-I-labeled RGCs in flat-mounted retinas (scale bar=100 μm) 4 weeks after increasing IOP. (A, B) Wild-type mice. (C, D) ApoE$^{-/-}$ mice. (A, C) Control. (B, D) Ocular hypertension. (E) Quantification of Di-I-labeled RGCs in wild-type and ApoE$^{-/-}$ mice after increasing IOP. $^{**}P<0.01$ compared to wild-type mice at the same time point ($n=8$ per time point).

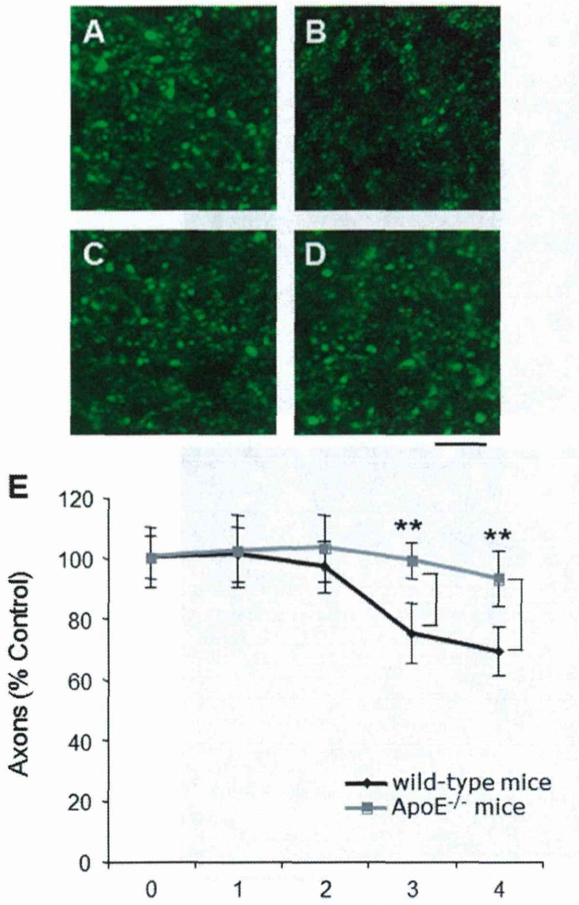

Fig. 4 – Time course of axonal degeneration after laser-induced ocular hypertension in both wild-type and ApoE$^{-/-}$ mice. (A–D) Representative photography showing the immunoreactivity of anti-phosphorylated neurofilaments in transverse sections of the optic nerve (scale bar = 10 μm) 4 weeks after increasing IOP. (A, B) Wild-type mice. (C, D) ApoE$^{-/-}$ mice. (A, C) Control. (B, D) Ocular hypertension. (E) Quantification of axon count in wild-type and ApoE$^{-/-}$ mice after increasing IOP. $^{**}P<0.01$ compared to wild-type mice at the same time point ($n=8$ per time point).

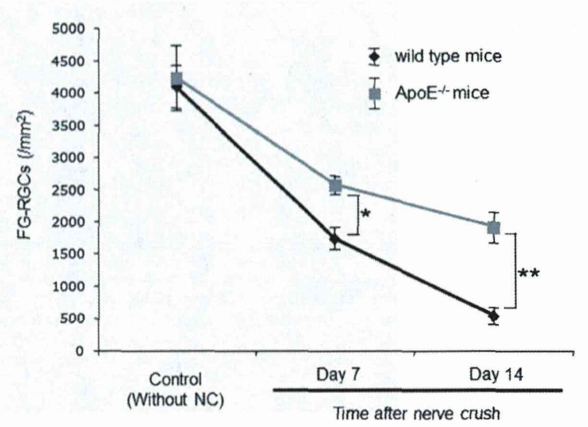

Fig. 5 – Time course of quantitative data for FG-labeled RGC death following nerve crush ($n=8$ per time point) in both wild-type and ApoE$^{-/-}$ mice. $^{*}P<0.05$ and $^{**}P<0.01$ compared to wild-type mice at the same time point.

(Himori et al., 2013), calpain activation (Ryu et al., 2012), and endoplasmic reticulum stress (Yasuda et al., 2014). In the current study, both KA-induced excitotoxicity and NC-induced RGC death were ameliorated in ApoE-deficient mice. Notably, CNQX, an inhibitor of the KA receptors, suppressed NC-induced RGC loss, but a suppresser of the NMDA receptors did not. This indicates that KA-induced excitotoxicity was significantly involved in RGC death in these mouse models. However, the details of this mechanism remain unclear, and further study is needed to understand the degree of crosstalk that may occur between the ApoE and KA pathways.

IHC showed that ApoE was localized in the astrocytes of both the retinas and optic nerves of mature mice. During the development of the mouse retina, the postnatal switchover of lipoprotein from ApoA-I to ApoE has been reported to occur after around 5–7 days (Kurumada et al., 2007). Additionally, ApoE was found to be localized in the Golgi apparatus in the cytosol of the astrocytes that secrete it (Boyles et al., 1985; Kurumada et al., 2007). ApoE and its receptor, LDL receptor-related protein (LRP1), have also been implicated in cellular differentiation, neuroprotection, and axonal growth of the RGCs (Hayashi et al., 2004; Hayashi et al., 2007; Hayashi et al., 2009; Hayashi et al., 2012). Furthermore, the retinal glial cells from ApoE-deficient mice were found not to induce the axonal elongation of the RGCs in vitro (Hayashi et al., 2004). These findings suggest that glia-derived ApoE and the subsequent activation of LRP1 play an important role in the development of the RGCs. Furthermore, the retinal structure of ApoE-deficient mice becomes severely degraded 35 weeks after birth (Ong et al., 2001; Ong et al., 2003). We therefore used 12-week-old mice, as their retinal structure remains intact. Interestingly, damage to the glial cells specifically caused by gliotoxin has also been found lead to subsequent damage to the retinal structure in WT mice (Jablonski and Iannaccone, 2000). In the central nervous system, astrocyte-derived ApoE has been shown to regulate brain homeostasis (Gee and Keller, 2005). These findings suggest that glia-derived ApoE has various beneficial effects that help RGCs to survive in adult mice.

In this study, we found that ApoE deficiency had a neuroprotective effect against damage caused by insults to the retina. This beneficial effect of ApoE remains difficult to explain. With advanced age, the glial cells of ApoE-deficient mice also become significantly damaged (Ong et al., 2001; Ong et al., 2003). One possible explanation of the neuroprotective effect of ApoE deficiency in mice is thus dysfunction of the glial cells. In the pathogenesis of OH-, NC-, and excitotoxicity-induced RGC death, astrocytes play a cytotoxic role in the RGCs, involving TNFα (Nakazawa et al., 2006), nitric oxide (Morgan, 2000), matrix metalloproteinase-9 (Zhang et al., 2004), tissue plasminogen activators, and urokinase plasminogen activators (Ganesh and Chintala, 2011). Recent reports have suggested that endogenous ApoE is distributed in the caveolin-1-rich domain (membrane raft), where the various receptors are located and intracellular signaling starts, along with the ATP-binding cassette

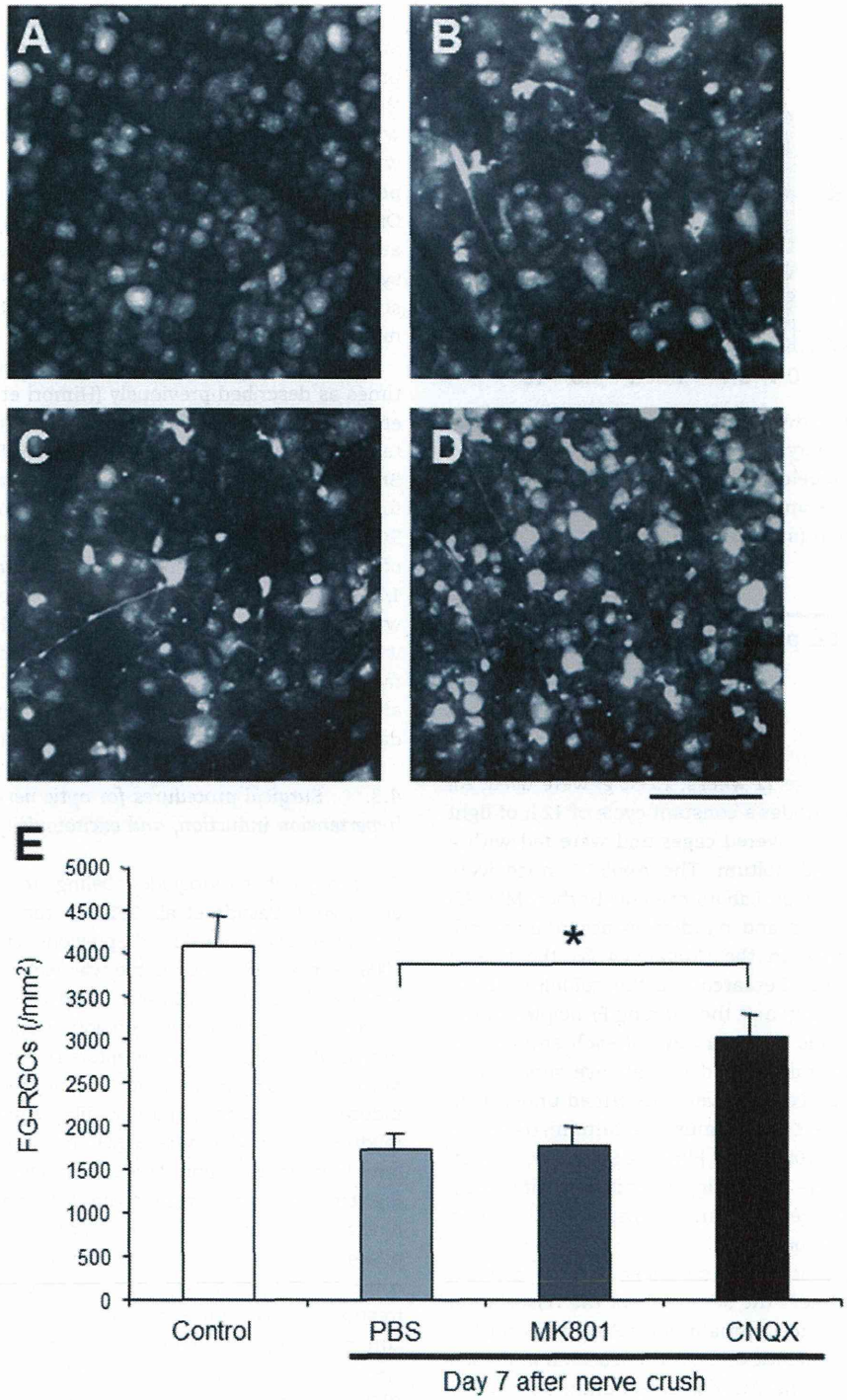

Fig. 6 – The neuroprotective effect of glutamate receptor antagonists in wild-type mice. (A-D) Representative photographs of FG-labeled RGCs in flat-mounted retinas (scale bar = 100 μm) 7 days after nerve crush. (A) Control. (B) PBS. (C) MK801. (D) CNQX. (E) Quantification of FG-labeled RGCs in wild-type mice 7 days after nerve crush. *$P < 0.05$ compared to PBS treatment.

transporter A1 in the astrocytes (Ito et al., 2014). Therefore, the dysfunction of glial cells induced by the deletion of ApoE, with its multipotential roles, may be related to the protective effect in damaged RGCs.

In conclusion, our studies in an experimental mouse model show that ApoE plays a critical role in the pathophysiological events that occur in ocular hypertension and after nerve crush. In ApoE-deficient mice, the cytotoxic pathways involving the KA receptors were suppressed. The blockade of KA-induced excitotoxicity, and possibly the upstream suppression of the astrocytes, may be an important future approach to the treatment of glaucoma.

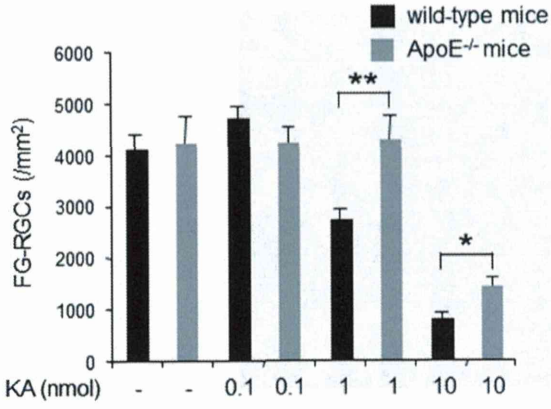

Fig. 7 – The neuroprotective effect of ApoE deficiency against KA-induced excitotoxicity in wild-type and ApoE$^{-/-}$ mice. Quantification of FG-labeled RGCs 7 days after nerve crush. *P<0.05 between wild-type and ApoE$^{-/-}$ mice with the same KA concentration (n=8 each).

4. Experimental procedure

4.1. Animals

In total, 124 male WT mice (C57BL/6, age 12 weeks, 23–27 g) and 96 ApoE$^{-/-}$ mice (age 12 weeks, 25–30 g) were used. All mice were maintained under a constant cycle of 12 h of light and 12 h of darkness in covered cages and were fed with a standard rodent diet ad libitum. The ApoE$^{-/-}$ mice were purchased from the Jackson Laboratory (Bar Harbor, ME). All animals were maintained and handled in accordance with the principles presented in the Guidelines for the Use of Animals in Neuroscience Research and the guidelines from the Declaration of Helsinki and the Guiding Principles in the Care and Use of Animals. The right eye of each animal was used as the experimental eye and the left eye served as a control. The surgical procedures were performed under deep anesthesia induced with the intramuscular administration of a mixture of ketamine (100 mg/kg, Phoenix Scientific, Inc., St. Joseph, MO) and xylazine (10 mg/kg, Phoenix Scientific, Inc.). All mice were euthanatized with an intraperitoneal injection of a lethal dose of pentobarbital.

All experimental procedures described in the present study were judged to meet the standards of the Association for Research in Vision and Ophthalmology Statement for the Use of Animals in Ophthalmic and Vision Research and used a protocol approved by the Animal Care Committee of the Ethics Committee for Animal Experiments at Tohoku University Graduate School of Medicine. All animals were treated according to the National Institutes of Health guidelines for the care and use of laboratory animals.

4.2. *Surgical procedure for retrograde labeling and RGC counting*

Seven days before the surgery, retrograde labeling with a solution containing 2% fluorogold (FG; Fluorochrome, LLC, Denver, Colorado) and 1% 1,1′-dioctadecyl-3,3,3′,3′-tetramethylindocarbocyanine perchlorate (Di-I, 468495, Sigma-Aldrich, St. Louis, MO) was performed as described previously (Himori et al., 2013; Nakazawa et al., 2006). Briefly, the animal was anesthetized and the skin over the cranium was incised to expose the scalp. A hole of 1 mm in diameter was made on each side of the skull with a drill 4 mm posterior to the bregma and 1 mm lateral to the midline. One microliter of the FG or Di-I solution was slowly injected at a 2 mm depth from the surface of skull with a Hamilton syringe equipped with 32G needle. The overlying skin was sutured with 6-0 nylon, and antibiotic ointment was externally applied.

FG- or Di-I-labeled RGCs were counted at various survival times as described previously (Himori et al., 2013; Nakazawa et al., 2006) under fluorescence microscopy (Leica Microsystems, Wetzlar, Germany) using a UV or Rhodamine filter set. Briefly, the retinas were fixed in 4% paraformaldehyde (PFA) for 2 h. Retinas were then flat-mounted onto glass slides, and RGCs labeled with FG or Di-I were counted in 12 distinct areas of 2.46×10^{-2} mm^2 each (three areas per retinal quadrant at 1/6, 3/6 and 5/6 of the retinal radius). The density of the RGCs was defined as an average value of the 12 fields. The counting was performed by two independent investigators in a masked fashion and the data were averaged. To count surviving RGCs after NC or the induction of OH, the retinas were harvested 7 days after NC or 30 days after OH induction.

4.3. *Surgical procedures for optic nerve crush, ocular hypertension induction, and excitotoxicity*

Seven days after retrograde labeling, an NC procedure (Himori et al., 2013; Yasuda et al., 2014) or the induction of OH were performed as described in our previous reports (Nakazawa et al., 2006). For NC, the optic nerve was exposed, crushed with fine forceps for 10 s and released. Blood circulation was then confirmed to be normal and antibiotic ointment was applied. To investigate the role of KA receptors in the RGCs of the NC eyes, MK801 or CNQX (Sigma) were administered intraperitoneally. To induce OH, the right pupil was dilated with a topically applied mixture of phenylephrine (5.0%) and tropicamide (0.8%) 10 min prior to laser irradiation. The anterior chamber was flattened by the removal of aqueous fluid, and laser photocoagulation of the limbus was performed with a 200 μm spot size and 100 mW laser power for 0.1 s. The laser beam was directly focused on the corneal limbus with 100±10 (mean±S.D.) confluent spots. After treatment, 0.1% atropine and an antibiotic ointment were administered to the cornea. IOP was measured weekly with applanation tonometry, as described previously (Matsubara et al., 2006), in both eyes over a 4-week period after laser irradiation. We excluded mice from the experimental group if their first measurement of IOP was not 30% above the baseline. Excitotoxicity was induced with the intravitreal administration of KA (0.1, 1, 10 nmol/eye) (Nakazawa et al., 2006; Nakazawa et al., 2008). Seven days after the administration of KA, the retinas were flat mounted and surviving FG-labeled RGCs were counted.

4.4. *Histological axon counting*

All quantitative analyses included at least 3 sections from each of 8 mice for each experimental condition. After extraction, the

optic nerve was immediately placed into a fixative consisting of 2.5% glutaraldehyde and 2% formaldehyde in 0.1 M cacodylate buffer with 0.08 M $CaCl_2$ overnight at 4 °C. The tissue was then washed in 0.1 M cacodylate buffer and postfixed in 2% aqueous OsO_4. The segments were dehydrated in graded alcohols and embedded in epon. One-micrometer sections were cut and stained with 1% toluidine blue in 1% borate buffer. The photomicrographs used for axon counting were taken at 5 fixed positions (center, superior, inferior, nasal and temporal) with an × 100 objective on a microscope (DMRXA, Leica). Axon counting was carried out in a masked fashion as previously described (Nakazawa et al., 2006).

4.5. *Immunohistochemistry*

Immunohistochemistry (IHC) was performed as previously described (Nakazawa et al., 2006, 2007a). Briefly, the eyes were surgically removed with the optic nerve still attached and fixed with 4% PFA overnight at 4 °C, and then cryoprotected with PBS containing 20% sucrose. Cryo-sections (thickness 10 μm) of the retina and optic nerve were mounted on the slides and incubated with blocking buffer (10% goat serum, 0.5% gelatin, 3% bovine serum albumin (BSA) and 0.2% Tween 20 in PBS). Next, they were incubated with rabbit anti-ApoE antibody (Biodesign, K23100R, 1:400), mouse anti-phosphorylated neurofilaments as a marker of surviving axons (Convance, SMI-31R, 1:500), mouse anti-glutamine synthetase as a marker of Müller cells (Chemicon, MAB302, 1:200), or mouse anti-GFAP as a marker of astrocytes (Simga, G3893, 1:200) overnight at 4 °C. Blocking buffers without primary antibodies served as negative controls. The sections were washed three times with PBST (PBS containing 0.2% Tween 20) and then incubated with an Alexa 488 or Alexa 568 secondary antibody (1:200, Invitrogen) for 1 h. The slides were washed three times and mounted with the VECTASHIELD Mounting Medium with DAPI (H-1200, Vector Laboratories, Burlingame, CA).

4.6. *Statistical analysis*

The data were analyzed with ANOVA followed by Scheffe's post-hoc test or Mann–Whitney *U*-tests with the software "EXCEL statistics" (SSRI, Tokyo, Japan). A p value <0.05 was considered statistically significant and is highlighted in all figures with an asterisk. All values are expressed as the mean ± standard deviation (SD).

Acknowledgments

No authors have any financial disclosures. The authors thank Mr. Tim Hilts for editing this manuscript. This paper was supported in part by JSPS KAKENHI Grants-in-Aid for Scientific Research (B) (T.N. 26293372), (C) (K.M. 26462677), and for Exploratory Research (T.N. 26670751, Y.T. 26670263).

REFERENCES

Amaratunga, A., Abraham, C.R., Edwards, R.B., Sandell, J.H., Schreiber, B.M., Fine, R.E., 1996. Apolipoprotein E is synthesized in the retina by Muller glial cells, secreted into the vitreous, and rapidly transported into the optic nerve by retinal ganglion cells. J. Biol. Chem. 271, 5628–5632.

Boyles, J.K., Pitas, R.E., Wilson, E., Mahley, R.W., Taylor, J.M., 1985. Apolipoprotein E associated with astrocytic glia of the central nervous system and with nonmyelinating glia of the peripheral nervous system. J. Clin. Invest. 76, 1501–1513.

Bu, G., 2009. Apolipoprotein E and its receptors in Alzheimer's disease: pathways, pathogenesis and therapy. Nat. Rev. Neurosci. 10, 333–344.

Collaborative Normal-Tension Glaucoma Study Group, 1998. The effectiveness of intraocular pressure reduction in the treatment of normal-tension glaucoma. Am. J. Ophthalmol. 126, 498–505.

De Castro, D.K., Punjabi, O.S., Bostrom, A.G., Stamper, R.L., Lietman, T.M., Ray, K., Lin, S.C., 2007. Effect of statin drugs and aspirin on progression in open-angle glaucoma suspects using confocal scanning laser ophthalmoscopy. Clin. Exp. Ophthalmol. 35, 506–513.

Ganesh, B.S., Chintala, S.K., 2011. Inhibition of reactive gliosis attenuates excitotoxicity-mediated death of retinal ganglion cells. PLoS One 6, e18305.

Gee, J.R., Keller, J.N., 2005. Astrocytes: regulation of brain homeostasis via apolipoprotein E. Int. J. Biochem. Cell Biol. 37, 1145–1150.

Hayashi, H., Campenot, R.B., Vance, D.E., Vance, J.E., 2004. Glial lipoproteins stimulate axon growth of central nervous system neurons in compartmented cultures. J. Biol. Chem. 279, 14009–14015.

Hayashi, H., Campenot, R.B., Vance, D.E., Vance, J.E., 2007. Apolipoprotein E-containing lipoproteins protect neurons from apoptosis via a signaling pathway involving low-density lipoprotein receptor-related protein-1. J. Neurosci. 27, 1933–1941.

Hayashi, H., Campenot, R.B., Vance, D.E., Vance, J.E., 2009. Protection of neurons from apoptosis by apolipoprotein E-containing lipoproteins does not require lipoprotein uptake and involves activation of phospholipase Cgamma1 and inhibition of calcineurin. J. Biol. Chem. 284, 29605–29613.

Hayashi, H., Eguchi, Y., Fukuchi-Nakaishi, Y., Takeya, M., Nakagata, N., Tanaka, K., Vance, J.E., Tanihara, H., 2012. A potential neuroprotective role of apolipoprotein E-containing lipoproteins through low density lipoprotein receptor-related protein 1 in normal tension glaucoma. J. Biol. Chem. 287, 25395–25406.

Heijl, A., Leske, M.C., Bengtsson, B., Hyman, L., Hussein, M., 2002. Reduction of intraocular pressure and glaucoma progression: results from the Early Manifest Glaucoma Trial. Arch. Ophthalmol. 120, 1268–1279.

Himori, N., Yamamoto, K., Maruyama, K., Ryu, M., Taguchi, K., Yamamoto, M., Nakazawa, T., 2013. Critical role of Nrf2 in oxidative stress-induced retinal ganglion cell death. J. Neurochem. 127, 669–680.

Honjo, M., Tanihara, H., Nishijima, K., Kiryu, J., Honda, Y., Yue, B.Y., Sawamura, T., 2002. Statin inhibits leukocyte-endothelial interaction and prevents neuronal death induced by ischemia-reperfusion injury in the rat retina. Arch. Ophthalmol. 120, 1707–1713.

Ito, J.I., Nagayasu, Y., Miura, Y., Yokoyama, S., Michikawa, M., 2014. Astrocytes endogenous apoE generates HDL-like lipoproteins using previously synthesized cholesterol through interaction with ABCA1. Brain Res..

Iwase, A., Suzuki, Y., Araie, M., Yamamoto, T., Abe, H., Shirato, S., Kuwayama, Y., Mishima, H.K., Shimizu, H., Tomita, G., Inoue, Y., Kitazawa, Y., 2004. The prevalence of primary open-angle

glaucoma in Japanese: the Tajimi Study. Ophthalmology 111, 1641–1648.
Jablonski, M.M., Iannaccone, A., 2000. Targeted disruption of Muller cell metabolism induces photoreceptor dysmorphogenesis. Glia 32, 192–204.
Kashiwagi, K., Ou, B., Nakamura, S., Tanaka, Y., Suzuki, M., Tsukahara, S., 2003. Increase in dephosphorylation of the heavy neurofilament subunit in the monkey chronic glaucoma model. Invest. Ophthalmol. Vis. Sci. 44, 154–159.
Kawaji, T., Inomata, Y., Takano, A., Sagara, N., Inatani, M., Fukushima, M., Tanihara, H., Honjo, M., 2007. Pitavastatin: protection against neuronal retinal damage induced by ischemia-reperfusion injury in rats. Curr. Eye Res. 32, 991–997.
Kim, C.S., Seong, G.J., Lee, N.H., Song, K.C., 2011. Prevalence of primary open-angle glaucoma in central South Korea the Namil study. Ophthalmology 118, 1024–1030.
Kurumada, S., Onishi, A., Imai, H., Ishii, K., Kobayashi, T., Sato, S.B., 2007. Stage-specific association of apolipoprotein A-I and E in developing mouse retina. Invest. Ophthalmol. Vis. Sci. 48, 1815–1823.
Lam, C.Y., Fan, B.J., Wang, D.Y., Tam, P.O., Yung Tham, C.C., Leung, D.Y., Ping Fan, D.S., Chiu Lam, D.S., Pang, C.P., 2006. Association of apolipoprotein E polymorphisms with normal tension glaucoma in a Chinese population. J. Glaucoma. 15, 218–222.
Levin, L.A., 2003. Retinal ganglion cells and neuroprotection for glaucoma. Surv. Ophthalmol. 48 (Suppl. 1), S21–S24.
Liang, Y.B., Friedman, D.S., Zhou, Q., Yang, X., Sun, L.P., Guo, L.X., Tao, Q.S., Chang, D.S., Wang, N.L., 2011. Prevalence of primary open angle glaucoma in a rural adult Chinese population: the Handan eye study. Invest. Ophthalmol. Vis. Sci. 52, 8250–8257.
Libby, R.T., Anderson, M.G., Pang, I.H., Robinson, Z.H., Savinova, O.V., Cosma, I.M., Snow, A., Wilson, L.A., Smith, R.S., Clark, A.F., John, S.W., 2005a. Inherited glaucoma in DBA/2J mice: pertinent disease features for studying the neurodegeneration. Vis. Neurosci. 22, 637–648.
Libby, R.T., Li, Y., Savinova, O.V., Barter, J., Smith, R.S., Nickells, R.W., John, S.W., 2005b. Susceptibility to neurodegeneration in a glaucoma is modified by Bax gene dosage. PLoS Genet. 1, 17–26.
Mabuchi, F., Tang, S., Ando, D., Yamakita, M., Wang, J., Kashiwagi, K., Yamagata, Z., Iijima, H., Tsukahara, S., 2005. The apolipoprotein E gene polymorphism is associated with open angle glaucoma in the Japanese population. Mol. Vis. 11, 609–612.
Mahley, R.W., 1988. Apolipoprotein E: cholesterol transport protein with expanding role in cell biology. Science 240, 622–630.
Marcus, M.W., Muskens, R.P., Ramdas, W.D., Wolfs, R.C., De Jong, P.T., Vingerling, J.R., Hofman, A., Stricker, B.H., Jansonius, N. M., 2012. Cholesterol-lowering drugs and incident open-angle glaucoma: a population-based cohort study. PLoS One 7, e29724.
Matsubara, A., Nakazawa, T., Husain, D., Iliaki, E., Connolly, E., Michaud, N.A., Gragoudas, E.S., Miller, J.W., 2006. Investigating the effect of ciliary body photodynamic therapy in a glaucoma mouse model. Invest. Ophthalmol. Vis. Sci. 47, 2498–2507.
Morgan, J.E., 2000. Optic nerve head structure in glaucoma: astrocytes as mediators of axonal damage. Eye 14 (Pt 3B), 437–444.
Nakazawa, T., Nakazawa, C., Matsubara, A., Noda, K., Hisatomi, T., She, H., Michaud, N., Hafezi-Moghadam, A., Miller, J.W., Benowitz, L.I., 2006. Tumor necrosis factor-alpha mediates oligodendrocyte death and delayed retinal ganglion cell loss in a mouse model of glaucoma. J. Neurosci. 26, 12633–12641.
Nakazawa, T., Hisatomi, T., Nakazawa, C., Noda, K., Maruyama, K., She, H., Matsubara, A., Miyahara, S., Nakao, S., Yin, Y., Benowitz, L., Hafezi-Moghadam, A., Miller, J.W., 2007a. Monocyte chemoattractant protein 1 mediates retinal detachment-induced photoreceptor apoptosis. Proc. Natl. Acad. Sci. USA 104, 2425–2430.
Nakazawa, T., Takahashi, H., Nishijima, K., Shimura, M., Fuse, N., Tamai, M., Hafezi-Moghadam, A., Nishida, K., 2007b. Pitavastatin prevents NMDA-induced retinal ganglion cell death by suppressing leukocyte recruitment. J. Neurochem. 100, 1018–1031.
Nakazawa, T., Shimura, M., Ryu, M., Nishida, K., Pages, G., Pouyssegur, J., Endo, S., 2008. ERK1 plays a critical protective role against N-methyl-D-aspartate-induced retinal injury. J. Neurosci. Res. 86, 136–144.
Ong, J.M., Zorapapel, N.C., Rich, K.A., Wagstaff, R.E., Lambert, R.W., Rosenberg, S.E., Moghaddas, F., Pirouzmanesh, A., Aoki, A.M., Kenney, M.C., 2001. Effects of cholesterol and apolipoprotein E on retinal abnormalities in ApoE-deficient mice. Invest. Ophthalmol. Vis. Sci. 42, 1891–1900.
Ong, J.M., Zorapapel, N.C., Aoki, A.M., Brown, D.J., Nesburn, A.B., Rich, K.A., Kenney, C.M., 2003. Impaired electroretinogram (ERG) response in apolipoprotein E-deficient mice. Curr. Eye Res. 27, 15–24.
Quigley, H.A., 1996. Number of people with glaucoma worldwide. Br. J. Ophthalmol. 80, 389–393.
Resnikoff, S., Pascolini, D., Etya'ale, D., Kocur, I., Pararajasegaram, R., Pokharel, G.P., Mariotti, S.P., 2004. Global data on visual impairment in the year 2002. Bull. World Health Organ. 82, 844–851.
Ressiniotis, T., Griffiths, P.G., Birch, M., Keers, S., Chinnery, P.F., 2004. The role of apolipoprotein E gene polymorphisms in primary open-angle glaucoma. Arch. Ophthalmol. 122, 258–261.
Ryu, M., Yasuda, M., Shi, D., Shanab, A.Y., Watanabe, R., Himori, N., Omodaka, K., Yokoyama, Y., Takano, J., Saido, T., Nakazawa, T., 2012. Critical role of calpain in axonal damage-induced retinal ganglion cell death. J. Neurosci. Res. 90, 802–815.
Schmitt, U., Sabel, B.A., 1996. MK-801 reduces retinal ganglion cell survival but improves visual performance after controlled optic nerve crush. J. Neurotrauma. 13, 791–800.
Schuettauf, F., Naskar, R., Vorwerk, C.K., Zurakowski, D., Dreyer, E.B., 2000. Ganglion cell loss after optic nerve crush mediated through AMPA-kainate and NMDA receptors. Invest. Ophthalmol. Vis. Sci. 41, 4313–4316.
Shanab, A.Y., Nakazawa, T., Ryu, M., Tanaka, Y., Himori, N., Taguchi, K., Yasuda, M., Watanabe, R., Takano, J., Saido, T., Minegishi, N., Miyata, T., Abe, T., Yamamoto, M., 2012. Metabolic stress response implicated in diabetic retinopathy: the role of calpain, and the therapeutic impact of calpain inhibitor. Neurobiol. Dis. 48, 556–567.
Suzuki, Y., Iwase, A., Araie, M., Yamamoto, T., Abe, H., Shirato, S., Kuwayama, Y., Mishima, H.K., Shimizu, H., Tomita, G., Inoue, Y., Kitazawa, Y., 2006. Risk factors for open-angle glaucoma in a Japanese population: the Tajimi Study. Ophthalmology 113, 1613–1617.
Tamura, H., Kawakami, H., Kanamoto, T., Kato, T., Yokoyama, T., Sasaki, K., Izumi, Y., Matsumoto, M., Mishima, H.K., 2006. High frequency of open-angle glaucoma in Japanese patients with Alzheimer's disease. J. Neurol. Sci. 246, 79–83.
Weinreb, R.N., Khaw, P.T., 2004. Primary open-angle glaucoma. Lancet 363, 1711–1720.
Yasuda, M., Tanaka, Y., Ryu, M., Tsuda, S., Nakazawa, T., 2014. RNA sequence reveals mouse retinal transcriptome changes early after axonal injury. PLoS One 9, e93258.
Zetterberg, M., Tasa, G., Palmer, M.S., Juronen, E., Teesalu, P., Blennow, K., Zetterberg, H., 2007. Apolipoprotein E polymorphisms in patients with primary open-angle glaucoma. Am. J. Ophthalmol. 143, 1059–1060.
Zhang, X., Cheng, M., Chintala, S.K., 2004. Kainic acid-mediated upregulation of matrix metalloproteinase-9 promotes retinal degeneration. Invest. Ophthalmol. Vis. Sci. 45, 2374–2383.

Journal of Neuroscience Research

Journal of Neuroscience Research 92:1637–1646 (2014)

Artemin Augments Survival and Axon Regeneration in Axotomized Retinal Ganglion Cells

Kazuko Omodaka,[1] Takuji Kurimoto,[2] Orie Nakamura,[1] Kota Sato,[1] Masayuki Yasuda,[1] Yuji Tanaka,[1] Noriko Himori,[1] Yu Yokoyama,[1] and Toru Nakazawa[1,3,4]*

[1]Department of Ophthalmology and Visual Science, Tohoku University Graduate School of Medicine, Sendai, Japan
[2]Department of Ophthalmology, Mimihara General Hospital, Sakai, Japan
[3]Department of Advanced Ophthalmic Medicine, Tohoku University Graduate School of Medicine, Sendai, Japan
[4]Department of Retinal Disease Control, Tohoku University Graduate School of Medicine, Sendai, Japan

Artemin, a recently discovered member of the glial cell line-derived neurotrophic factor (GDNF) family, has neurotrophic effects on damaged neurons, including sympathetic neurons, dopamine neurons, and spiral ganglion neurons both in vivo and in vitro. However, its effects on retinal cells and its intracellular signaling remain relatively unexplored. During development, expression of GFRα3, a specific receptor for artemin, is strong in the immature retina and gradually decreases during maturation, suggesting a possible role in the formation of retinal connections. Optic nerve damage in mature rats causes levels of GFRα3 mRNA to increase tenfold in the retina within 3 days. GFRα3 mRNA levels continue to rise within the first week and then decline. Artemin, a specific ligand for GFRα3, has a neuroprotective effect on axotomized retinal ganglion cells (RGCs) in vivo and in vitro via activation of the extracellular signal-related kinase– and phosphoinositide 3-kinase–Akt signaling pathways. Artemin also has a substantial effect on axon regeneration in RGCs both in vivo and in vitro, whereas other GDNF family members do not. Therefore, artemin/GFRα3, but not other GDNF family members, may be of value for optic nerve regeneration in mature mammals.

Key words: retinal ganglion cell; regeneration; growth factor; signal transduction; mitogen-activated protein kinase; optic nerve axotomy; glaucoma

Glial cell line-derived neurotrophic factor (GDNF) was initially identified as a factor secreted from a glioma cell line that can support the survival of embryonic ventral midbrain neurons in culture (Lin et al., 1993). Subsequent studies have shown that GDNF is an important trophic factor for multiple types of neurons and glia (Baloh et al., 2000). Additional members of the GDNF family have since been identified (Lindahl et al., 2000; Carmillo et al., 2005) and include neurturin (NRTN), artemin (ARTN), and persephin (PSPN). GDNF family ligands activate the receptor tyrosine kinase Ret through binding of glycosylphosphatidylinositol-anchored GDNF family receptor α (GFRα) coreceptors 1–4 (Sariola and Saarma, 2003). GDNF binds GFRα1, NRTN binds GFRα2, ARTN binds GFRα3, and PSPN binds GFRα4 (Lindahl et al., 2000; Carmillo et al., 2005). These receptors have no kinase domain but act through the associated Ret tyrosine kinase, leading to Ret autophosphorylation and the initiation of intracellular signaling. Downstream signaling includes the activation of mitogen-activated protein kinase (MAPK), phosphoinositide 3-kinase (PI3K)–AKT, phospholipase Cγ, cAMP response element-binding (CREB), and Src-family kinases (SFK) pathways (Trupp et al., 1999; Baloh et al., 2000; Jeong et al., 2008). In addition, GFRs can potentially activate CREB directly through a Ret-independent mechanism (Trupp et al., 1999). The regulation of GFR expression would be expected to play a pivotal role in controlling ligand-mediated effects. For example, GFRα3 is highly expressed on embryonic day 11 but is not appreciably expressed in adult mouse of dorsal root ganglia (DRG) or superior cervical sympathetic ganglion (SCG; Worby et al., 1998).

Contract grant sponsor: JSPS Grants-in-Aid for Scientific Research (B), contract grant number: 26293372 (to T.N.); Contract grant sponsor: JSPS Grants-in-Aid for Exploratory Research, contract grant numbers: 26670751 (to T.N.); 26670263 (Y.T.); Contract grant sponsor: JSPS Grants-in-Aid for Young Scientists, contract grant number: 26861434 (to N.H.).

*Correspondence to: Toru Nakazawa, MD, PhD, Department of Ophthalmology, Tohoku University Graduate School of Medicine, 1-1, Seiryo, Aoba, Sendai, Miyagi 980-8574, Japan.
E-mail: ntoru@fa2.so-net.ne.jp

Received 17 April 2014; Revised 3 June 2014; Accepted 10 June 2014

Published online 9 July 2014 in Wiley Online Library (wileyonlinelibrary.com). DOI: 10.1002/jnr.23449

GDNF, NRTN, and PSPN exert neuroprotective effects on injured neurons through the PI3K–Akt signaling pathway. This pathway has been shown to be important in preventing the death of retinal ganglion cells (RGCs) in various pathological conditions (Nakazawa et al., 2002b, 2003, 2005b). In isolated retinal Muller glial cells, stimulation of GDNF-family protein resulted in the transcriptional upregulation of FGF-2 (Hauck et al., 2006). Although the roles of GDNF-GFRα1 and NRTN-GFRα2 have been characterized to some extent in the visual system (Hauck et al., 2006; Brantley et al., 2008; Koeberle and Bahr, 2008), the roles of ARTN and GFRα3 remain unknown.

This study examined the changes in expression of growth factor receptors after optic nerve axotomy and showed that GFRα3 receptors were selectively upregulated. We also investigated the role of GDNF-family receptor genes in retinal development, in the optic nerve following axotomy, and in retinal primary cultures. Our data suggest that GDNF-family proteins have a substantial neuroprotective effect on RGCs and that ARTN, a recently discovered member of the GDNF family, has unique effects on axon regeneration.

MATERIALS AND METHODS

Animals and Surgical Procedure

One hundred thirty-six male Sprague-Dawley rats (SLC, Hamamatsu, Japan) weighing 200–240 g were used in this study. All animals were maintained and handled in accordance with the ARVO Statement for the Use of Animals in Ophthalmic and Vision Research.

Transection of the optic nerve was performed on the right eye as previously described (Nakazawa et al., 2002a,b). In brief, rats were anesthetized via intraperitoneal injection of sodium pentobarbital (Nembutal; 45 mg/kg of body weight), and the optic nerve was transected about 1 mm posterior to the eyeball, with care taken not to damage the retinal blood supply. To identify RGCs in the ganglion cell layer (GCL), we performed retrograde labeling by placing a small piece of gelfoam soaked with 2% aqueous Fluorogold (FG; Fluorochrome, Englewood, CO) containing 1% dimethylsulfoxide (DMSO) at the optic stump after optic nerve axotomy. Fifteen minutes before optic nerve surgery, 1 μg of GDNF, NRTN, or ARTN (Peprotech, Rocky Hill, NJ) in phosphate-buffered saline (PBS; 3 μl) containing 0.1% bovine serum albumin (BSA) was injected intravitreally by puncturing the eyeball at the cornea–sclera junction with a 32-G needle on a Hamilton syringe. Animals were excluded if the lens was injured during the course of intraocular injection.

For the in vivo experiment for axon regeneration, the optic nerve was crushed as previously described (Kurimoto et al. 2006, 2010). The animal was anesthetized with 7% chloral hydrate solution (400 mg/kg). After skin incision, the left optic nerve was exposed and mechanically crushed with jewelry forceps (Dumont No. 545; World Precision Instruments, Tokyo, Japan) for 10 sec, 2 mm behind the eye. We verified, with a direct ophthalmoscope, that the integrity of the retinal blood supply was not damaged. To investigate the effect of GDNF, NRTN, and ARTN on axon regeneration, all reagents were injected into the vitreous with a glass micropipette through a hole made by a 27-G needle on days 0, 1, 4, and 7.

Twelve days after the optic nerve was crushed, the operated animals were anesthetized with a 7% chloral hydrate solution, and 3 μl 1% cholera toxin B subunit solution (CTB; List Biological Laboratories, Campbell, CA) was intravitreally injected. Two days after the CTB application, the animals were transcardially perfused with 4% paraformaldehyde (PFA) in phosphate buffer. The optic nerve was dissected and immersed in 30% sucrose for cryoprotection, and then it was sectioned longitudinally at a thickness of 16 μm. After being blocked, the sections were incubated by 1:4,000 goat anti-CTB antibody (List Biological Laboratories) and in 1:200 biotinylated rabbit anti-goat IgG antibody (Vector Laboratories, Burlingame, CA) for 2 hr at room temperature (RT), followed by 1:400 Alexa 488-conjugated streptavidin (Molecular Probes, Eugene, OR). The sections were then mounted with antifade reagent (Molecular Probes), and axons were counted as previously described (Kurimoto et al., 2006). Under fluorescent microscopy (Optishot; Leica, California), CTB-labeled axons were directly counted at each grid line 250, 500, or 1,000 μm from the distal end of the crush site. The mean number of axons at each distance was calculated from seven to 10 sections per animal.

RNA Extraction and Quantitative Reverse Transcription-Polymerase Chain Reaction

RNA extraction and real-time reverse transcription-polymerase chain reaction (RT-PCR) were performed as previously described (Nakazawa et al., 2000), with minor modification. Retinas were directly lysed in Qiagen (Hilden, Germany) RNeasy RLT lysis buffer. Subsequent RNA extraction was performed with the RNeasy microkit (Qiagen) according to the manufacturer's instructions. Total RNA (200 ng) was reverse transcribed by using a SuperScript III first strand synthesis kit (Life Technologies, Frederick, MD) to synthesize cDNA. First-strand cDNA was amplified by using the Expand Long Template PCR system (Boehringer Mannheim, Indianapolis, IN), with PCR primer sets for GFRα1 5′-TGG CAGCCAGCCCCTCCAGTCCA-3′ and 5′-TTGGGTG AAACTGCTTCTCAACG-3′, GFRα2 5′-TCTCCCAAA GGCCCCTCACTCCCA-3′ and 5′-ATGTGTGTATGCGTG TGTTTCCA-3′, GFRα3 5′-GAGCATGCTCAAACCAGACT CCGA-3′ and 5′-TGTGGAAACGCATTTTAGCCGCAA-3′, and Ret 5′-TGGGCCAGTATCTCTATGGCGTCT-3′. RT-PCR of 18S ribosomal RNA (5′-CATGCATGTCTAAGTACG CACGG-3′ and 5′-CGGCGACTACCATCGAAAGTTGA-3′) was used as an internal control for the reactions. PCR amplification was performed by using the GeneAmp PCR System 2400 (Perkin Elmer/Applied Biosystems, Waltham, MA) for the number of cycles indicated as GFRα1 (24 cycles), GFRα2 (24 cycles), GFRα3 (28 cycles), Ret (24 cycles), and 18S (10 cycles) with denaturation at 96°C for 30 sec, annealing at 60°C for 30 sec, and extension at 72°C for 90 sec, followed by extension at 72°C for 7 min. PCR products were evaluated by agarose gel electrophoresis followed by staining with ethidium bromide and sequencing. The gel was photographed by using short wave-length UV, and the fluorescent intensity of the product bands was determined by

densitometry. To ensure that measurements were in a linear range, the intensity of the PCR product bands of several cycles was measured by densitometry and plotted to determine its linear range of amplification (data not shown). The data presented were all in the linear range.

For the real-time quantitative PCR, first-strand cDNA was amplified with a 7500 fast real-time PCR system (Applied Biosystems, Foster City, CA) with Taqman probe sets (Life Technologies) for GFRα1 (Rn01444617_m1), GFRα2 (Rn00562583_m1), GFRα3 (Rn01760829_m1), Ret (Rn01463098_m1), and glyceraldehyde-3-phosphate dehydrogenase (GAPDH; Rn01462662_g1). Relative gene expression levels were calculated by using the ΔΔCt method.

Counting FG-labeled RGCs in Retinal Flat Mounts

Preparation of whole-mounted retina was as previously described (Nakazawa et al., 2002a,b). Rats were sacrificed by an overdose of Nembutal 10 days after optic nerve transection. Retinas were dissected, fixed in 4% PFA. and flat mounted onto glass slides. RGC densities were determined by counting FG-labeled RGCs in 12 distinct areas, each measuring 7.29×10^{-2} mm^2 (three areas per quadrant at 1/6, 3/6, and 5/6 of the distance from the optic nerve head to the periphery along a retinal radius). The density of FG RGCs was defined as the average value of the 12 fields counted and analyzed statistically, as previously described (Nakazawa et al., 2002a,b). The counting of FG-labeled RGCs was conducted under microscopy in a masked fashion by two independent investigators.

Immunoblot and Immunohistochemistry

Three days after treatment with or without axotomy, the retinas were isolated and placed into a sampling buffer as HBS (pH 7.4) containing 1% protease inhibitor cocktail (Sigma-Aldrich, St. Louis, MO) and homogenized in lysis buffer as HBST (0.5% Triton X-100, pH 7.4) containing 1% protease inhibitor cocktail. Cell lysates were clarified by centrifugation at 15,000*g* at 4°C for 20 min. Each cell lysate was collected into a new tube, and quantity of protein concentration was determined by using a BCA kit (ThermoFisher Scientific, Rockford, IL). For each sample, 10 μg total protein was applied per lane, separated with sodium dodecyl sulfate-polyacrylamide gel electrophoresis, and electroblotted onto a polyvinylidene fluoride (PVDF) membrane (Millipore, Bedford, MA). After nonspecific binding had been blocked with 8% Block Ace (Yukijirushi, Sapporo, Japan), the membranes were incubated at 4°C overnight with a rabbit polyclonal antibody against GFRα3 (1:1,000, ab-8028; Abcam, Cambridge, MA) and β-actin (1:5,000, A5316; Sigma-Aldrich). The membranes were then incubated with a horseradish peroxidase-conjugated anti-rabbit or anti-mouse immunoglobulin secondary antibody for 1 hr. The signals were visualized with chemiluminescence (ECL prime blotting analysis system; GE Healthcare, Tokyo, Japan), measured in Image Lab statistical software (Bio-Rad, Hercules, CA), and normalized to β-actin.

Immunohistochemistry was performed as previously described (Nakazawa et al., 2002a,b). Briefly, surgically removed retinas were fixed with 4% PFA at 4°C overnight and then cryoprotected with PBS, 0.1 M phosphate buffer (pH 7.4), and 0.15 M NaCl containing 20% sucrose. Cryosections (10 μm) were mounted on slides and incubated with blocking buffer (10% goat serum, 0.5% gelatin, 3% BSA, and 0.2% Tween-20 in PBS) for 1 hr. Then the sections were incubated with blocking buffer and a primary antibody made in rabbit against GFRα3 (AB5400; Chemicon, Temecula, CA). Normal serum (Dako, Osaka, Japan) was used as a negative control. The sections were then incubated with Alexa TM 488-labeled secondary antibody (1:200 in blocking buffer; Molecular Probes) for 1 hr. Slides were washed three times with PBS containing 0.2% Tween-20 and mounted with Vectashield mounting media with 4′,6-diamidino-2 phenylindole (DAPI; Vector Laboratories). Photographs of the retina were taken routinely at an area 1 mm from the center of the optic nerve with a fluorescent microscope (Qfluoro system; Leica Microsystems, Wetzlar, Germany) with a UV filter (DAPI) and an FITC filter (immunostaining).

For double staining with GFRα3 and Brn3a, retinal sections were sliced (12 μm thick) with a cryostat and collected on MES-coated slides (Matsunami, Osaka, Japan). For the immunohistochemistry procedure, sections were blocked with 10% normal serum and 1% Triton X-100 in PBS for 1 hr at RT and then reacted with primary antibodies rabbit anti-GFRα3 (1:50, ab8028; Abcam) and mouse anti-Brn3a (1:200, sc-8429; Santa Cruz Biotechnology, Santa Cruz, CA) overnight at 4°C. After being washed in PBS, the sections were incubated with Alexa TM 488 (GFRα3)- or 568 (Brn3a)-labeled secondary antibodies for 1 hr at RT and mounted on Vectashield mounting media with DAPI. The sections were analyzed with a Leica TCS SP2 laser scanning spectral confocal microscope.

Adult Rat Retinal Primary Cultures

Adult primary retinal cultures were prepared as previously described (Yin et al., 2006; Nakazawa et al., 2007). Cells from two retinas were resuspended in 1 ml Neurobasal A medium (Invitrogen, Carlsbad, CA) containing B27 supplement (Invitrogen) with antioxidants for axonal growth analysis (NBA/B27AO$^+$) or without antioxidants for cell survival assay (NBA/B27AO$^-$), and cells were counted by using a hemocytometer after incubation with the same volume of 0.4% Trypan blue solution (Sigma). Cell density was adjusted to 4×10^5 cells/ml with culture medium, and 100 μl cell suspension was seeded into each well of an eight-well chamber (Nunc; 4×10^4 cells per well). Ten minutes after seeding the cells, the total volume in each well was brought up to 400 μl by adding 300 μl of culture medium containing 1 μg/ml insulin, 2 mM L-glutamate, and 12 μg/ml gentamycin. One hour later, GDNF, NRTN, and ARTN at specified concentrations were added to the culture medium, and incubation continued in a 5% CO_2 atmosphere at 37°C for 24 hr for cell survival assay or for 72 hr for axonal growth analysis. Cells were then gently washed with PBS and fixed with 4% PFA for 10 min at RT. To assess the viability of RGCs, we performed immunocytochemistry with mouse anti-β3-tubulin antibody, an RGC marker (Nakazawa et al., 2007). Briefly, cells were permeabilized with 0.1% Triton X-100 in PBS for 5 min and blocked by blocking buffer for 30 min at RT. Cells were then incubated with a monoclonal anti-β3-tubulin antibody (1:150 dilution; Sigma) at RT for 2 hr, rinsed with PBS (3 × 5 min), incubated with goat anti-mouse